

Quantum correlation and entanglement between an ionizing system and a neighbor atom interacting directly and via a quantized field

V. Peřinová,^{1,*} A. Lukš,¹ J. Křepelka,¹ and J. Peřina, Jr.²

¹*Joint Laboratory of Optics, Palacký University, RCPTM,
17. listopadu 12, 77146 Olomouc, Czech Republic*

²*Institute of Physics of Academy of Sciences of the Czech Republic,
Joint Laboratory of Optics, Palacký University, RCPTM,
17. listopadu 12, 77146 Olomouc, Czech Republic*

(Dated:)

Quantum correlations between two neighbor atoms are studied. It is assumed that one atomic system comprises a single auto-ionizing level and the other atom does not contain any auto-ionizing level. The excitation of both atoms is achieved by the interaction with the same mode of the quantized field. It is shown that the long-time behavior of two atoms exhibits quantum correlations even when the atoms do not interact directly. This can be shown using the optical excitation of the neighbor atom. Also a measure of entanglement of two atoms can be applied after reduction of the continuum to two levels.

PACS numbers: 32.80.-t, 33.80.Eh, 34.20.-b

I. INTRODUCTION

In the study of atoms with at least two electrons, bound states and resonances are of interest. The resonances evolve into states with one free electron after a very short time. This phenomenon is called auto-ionization of the atom. With a revival of interest in the auto-ionization, Fano published an appealing theoretical paper [1] comprising an analysis of the excitation of the $2s2p$ level of helium by electrons. He argued that the natural line shape contains a zero. Later, the optical absorption spectra of the rare gases have been analyzed [2], while the paper [3] is one of many studies dealing with the mechanism of atomic auto-ionization. A unified approach to the configuration interaction and the influence of strong lasers have been expounded in [4]. In this framework, the studies [5, 6] have been realized. The quantum laser field has been taken into account in [7] and the effect of the squeezed state has been studied in [8].

The Fano resonances can occur also in other physical settings. The Fano resonances in nanoscale structures can be mentioned [9]. The treatment of auto-ionization and the influence of laser may be extended to a simultaneous auto-ionization, the influence of laser, and to the interaction with a neighbor two-level atom [10–14]. The presence of a neighbor system may also considerably increase photo-ionization and recombination rates [15, 16]. In the analysis, the assumption of weak optical pumping is usually used and leads to a simpler behavior, cf., [4].

In [17], the entanglement between an auto-ionization system and a neighbor atom is studied for a classical driving field. Besides the possibility to calculate a measure of entanglement for the two atomic systems, a somewhat

arbitrary, but systematic, filtering is adopted. Two frequencies can be selected in the auto-ionization system and the study of entanglement reduces to the well-known two-qubit problem. In this paper, we modify this analysis by including the quantal nature of the field. In Sec. II, we describe the model. In Sec. III, we discuss photoelectron spectra and the density plots of entanglement measure. Sec. IV provides conclusion.

II. QUANTUM MODEL OF THE OPTICAL EXCITATION OF TWO ATOMS

We consider two mutually interacting atoms, a and b , in the presence of an electromagnetic field (for the scheme, see Fig. 1). To quantize the electromagnetic field, we have to add to the usual model annihilation and creation operators of the modes which participate in the radiative interactions. Indeed, although only the frequency ω_L of optical field is considered, an infinity of modes at this frequency can be introduced.

We may suppose that the atom a interacts with the mode L_a and the atom b interacts with the mode L_b . We complete the levels of the atomic system by the photon-number states,

$$\begin{aligned} &|n_a, n_b\rangle_L \otimes |0, 0\rangle_{ab}, |n_a - 1, n_b\rangle_L \otimes |1, 0\rangle_{ab}, \\ &|n_a, n_b - 1\rangle_L \otimes |0, 1\rangle_{ab}, |n_a - 1, n_b - 1\rangle_L \otimes |1, 1\rangle_{ab}, \\ &|n_a, n_b - 1\rangle_L \otimes |0, E_d\rangle_{ad}, \\ &|n_a - 1, n_b - 1\rangle_L \otimes |1, E_d\rangle_{ad}, \end{aligned} \quad (1)$$

where n_a is a photon number in the mode L_a and n_b is a photon number in the mode L_b . In Eq. (1), $|0\rangle_a$ ($|0\rangle_b$) is the ground state of the atom a (b), $|1\rangle_a$ is the excited state of the atom a , $|1\rangle_b$ is the auto-ionization state of the atom b , $|E_d\rangle \equiv |E_d\rangle_d$ is the continuum state of the atom b , and E_d is an energy difference between the ground state $|0\rangle_b$ and the state $|E_d\rangle$. Here we have used

*Electronic address: vlasta.perinova@upol.cz

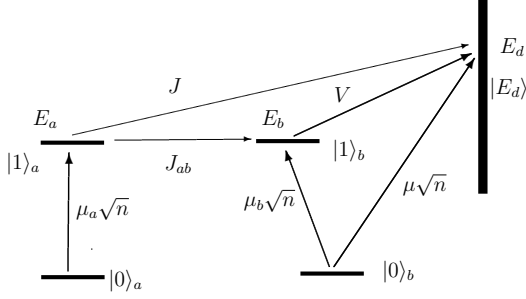


FIG. 1: Sketch of an auto-ionization system b interacting with a two-level atom a through a quantized field in the Fock state $|n\rangle$. The ground (excited) states are denoted as $|0\rangle_a$ and $|0\rangle_b$ ($|1\rangle_a$, $|1\rangle_b$, and $|E_d\rangle$). The dipole moments μ_a , μ_b , and μ describe the interactions between atoms and field. The excited discrete state of atom a (b) has the energy E_a (E_b), whereas the energies E_d characterize the excited states $|E_d\rangle$ of the continuum. Symbol V stands for the Coulomb configurational coupling between the excited states of atom b . The constants J_{ab} and J describe the dipole-dipole interaction between the atoms a and b .

the photon-number states $|n_a\rangle$, $|n_b\rangle$, $|n_a - 1\rangle$, and $|n_b - 1\rangle$ simultaneously to indicate that the Hilbert space of the states can be decomposed into invariant subspaces. For $n_a, n_b \geq 1$, these subspaces have a dimension equal to 6. Each invariant subspace is a tensorial product of the subspaces corresponding to the Jaynes–Cummings model (dimension 2) and the model due to Leoński and Bużek (dimension 3) [7]. The Hamiltonian has the form

$$\hat{H} = \hat{H}'_{\text{free}} + \hat{H}'_{a-i} + \hat{H}_{t-a} + \hat{H}_{\text{trans}}, \quad (2)$$

where

$$\hat{H}'_{\text{free}} = \hbar\omega_L(\hat{a}_L^\dagger\hat{a}_L + \hat{b}_L^\dagger\hat{b}_L), \quad (3)$$

with \hat{a}_L and \hat{b}_L (\hat{a}_L^\dagger and \hat{b}_L^\dagger) being the photon annihilation (creation) operators. The Hamiltonian \hat{H}'_{a-i} of atom b with auto-ionizing level in Eq. (2) is written as

$$\begin{aligned} \hat{H}'_{a-i} &= E_b|1\rangle_{bb}\langle 1| + \int E_d|E_d\rangle\langle E_d| dE_d \\ &+ \int (V|E_d\rangle_b\langle 1| + \text{H.c.}) dE_d \\ &+ (\mu_b\hat{b}_L|1\rangle_{bb}\langle 0| + \text{H.c.}) \\ &+ \int (\mu\hat{b}_L|E_d\rangle_b\langle 0| + \text{H.c.}) dE_d, \end{aligned} \quad (4)$$

where E_b means an energy difference between the ground state $|0\rangle_b$ and the state $|1\rangle_b$. Symbol μ_b gives the strength of optical excitation from the ground state $|0\rangle_b$ into the auto-ionization state $|1\rangle_b$, μ is the strength of optical excitation from the ground state $|0\rangle_b$ of the atom b into the continuum state $|E_d\rangle$, and V describes the Coulomb configuration interaction between the excited states of atom

b . The Hamiltonian of the neighbor two-level atom in Eq. (2) reads

$$\hat{H}_{t-a} = E_a|1\rangle_{aa}\langle 1| + (\mu_a\hat{a}_L|1\rangle_{aa}\langle 0| + \text{H.c.}), \quad (5)$$

where E_a means an energy difference between the ground state $|0\rangle_a$ and the state $|1\rangle_a$, μ_a is the strength of optical excitation from the ground state $|0\rangle_a$ into the excited state $|1\rangle_a$.

In Eq. (2), the Hamiltonian \hat{H}_{trans} characterizes the dipole–dipole interaction between the atoms a and b ,

$$\begin{aligned} \hat{H}_{\text{trans}} &= (J_{ab}|1\rangle_{bb}\langle 0||0\rangle_{aa}\langle 1| + \text{H.c.}) \\ &+ \int (J|E_d\rangle_b\langle 0||0\rangle_{aa}\langle 1| + \text{H.c.}) dE_d, \end{aligned} \quad (6)$$

where J_{ab} (J) characterize energy transfer from the ground state $|0\rangle_b$ into the state $|1\rangle_b$ ($|E_d\rangle$) at the cost of the decay from the state $|1\rangle_a$ into the state $|0\rangle_a$. We note that if $J_{ab} = 0$ and $J = 0$, the Hamiltonian \hat{H} describes uncoupled atoms.

We will treat the situation where the atoms a and b interact with a single mode L , $\hat{b}_L \rightarrow \hat{a}_L$. In this case, the levels written in Eq. (1) simplify,

$$\begin{aligned} &|n\rangle_L \otimes |0, 0\rangle_{ab}, |n-1\rangle_L \otimes |1, 0\rangle_{ab}, \\ &|n-1\rangle_L \otimes |0, 1\rangle_{ab}, |n-2\rangle_L \otimes |1, 1\rangle_{ab}, \\ &|n-1\rangle_L \otimes |0, E_d\rangle_{ad}, |n-2\rangle_L \otimes |1, E_d\rangle_{ad}, \end{aligned} \quad (7)$$

and n is the number of photons in the mode L . Here we have used the photon-number states $|n\rangle_L$, $|n-1\rangle_L$, and $|n-2\rangle_L$ simultaneously to indicate that the Hilbert space of the states can be decomposed into invariant subspaces. But in the case of a single mode, an invariant subspace cannot be investigated as a tensorial product. We can see from Eq. (7), that the atom a at the level $|0\rangle_a$ interacts with the field in the state $|n\rangle_L$ or $|n-1\rangle_L$ in the dependence on the state of the atom b and the atom a at the level $|1\rangle_a$ interacts with the field in the state $|n-1\rangle_L$ or $|n-2\rangle_L$ in the dependence on the state of the atom b .

The Hamiltonian has the form

$$\hat{H} = \hat{H}'_{\text{free}} + \hat{H}_{a-i} + \hat{H}_{t-a} + \hat{H}_{\text{trans}} \quad (8)$$

where

$$\hat{H}'_{\text{free}} = \hbar\omega_L\hat{a}_L^\dagger\hat{a}_L \quad (9)$$

and

$$\hat{H}_{a-i} = \hat{H}'_{a-i}\Big|_{\hat{b}_L \rightarrow \hat{a}_L}. \quad (10)$$

Following [7], we modify the Schrödinger picture by considering the state vector $|\psi\rangle(t)$ in the form

$$\begin{aligned} |\psi\rangle(t) &= \sum_{n=0}^{\infty} \exp\left[-\frac{i}{\hbar}E_L(n-2)t\right] \\ &\times \left[c_{00}^{(n)}(t)|n\rangle_L|0, 0\rangle_{ab} + c_{10}^{(n-1)}(t)|n-1\rangle_L|1, 0\rangle_{ab} \right] \end{aligned}$$

$$\begin{aligned}
& + c_{01}^{(n-1)}(t)|n-1\rangle_L|0,1\rangle_{ab} \\
& + c_{11}^{(n-2)}(t)|n-2\rangle_L|1,1\rangle_{ab} \\
& + \int d_0^{(n-1)}(E_d, t)|n-1\rangle_L|0, E_d\rangle_{ad} dE_d \\
& + \int d_1^{(n-2)}(E_d, t)|n-2\rangle_L|1, E_d\rangle_{ad} dE_d \Big], \quad (11)
\end{aligned}$$

where $E_L = \hbar\omega_L$. The prime indicates that for $n = 0, 1$ some of the components must be omitted. The components with $|n-2\rangle_L$ have to be omitted for $n = 0, 1$ and those with $|n-1\rangle_L$ have to be left out for $n = 0$.

It holds that $[\hat{J}, \hat{H}] = \hat{0}$ for

$$\hat{J} = |1\rangle_b \langle 1| + \int |E_d\rangle \langle E_d| dE_d + |1\rangle_a \langle 1| + \hat{a}_L^\dagger \hat{a}_L. \quad (12)$$

An invariant subspace $\mathcal{H}^{(n)}$ is the eigenspace of the operator \hat{J} related to an eigenvalue n . We assume that $n \geq 2$. In this invariant subspace, the composite system is described by the equations

$$\begin{aligned}
\frac{d}{dt} \mathbf{c}^{(n)}(t) &= -\frac{i}{\hbar} \mathbf{A}^{(n)} \mathbf{c}^{(n)}(t) \\
&\quad - \frac{i}{\hbar} \int \mathbf{B}_1^{(n)} \mathbf{d}^{(n)}(E_d, t) dE_d, \\
\frac{d}{dt} \mathbf{d}^{(n)}(E_d, t) &= -\frac{i}{\hbar} \mathbf{B}_2^{(n)} \mathbf{c}^{(n)}(t) \\
&\quad - \frac{i}{\hbar} \mathbf{K}^{(n)}(E_d) \mathbf{d}^{(n)}(E_d, t), \quad (13)
\end{aligned}$$

where

$$\begin{aligned}
\mathbf{c}^{(n)}(t) &= \begin{pmatrix} c_{00}^{(n)}(t) \\ c_{10}^{(n-1)}(t) \\ c_{01}^{(n-1)}(t) \\ c_{11}^{(n-2)}(t) \end{pmatrix}, \\
\mathbf{d}^{(n)}(E_d, t) &= \begin{pmatrix} d_0^{(n-1)}(E_d, t) \\ d_1^{(n-2)}(E_d, t) \end{pmatrix}. \quad (14)
\end{aligned}$$

Further

$$\mathbf{A}^{(n)} = \begin{pmatrix} 2E_L & \mu_a^* \sqrt{n} & \mu_b^* \sqrt{n} & 0 \\ \mu_a \sqrt{n} & E_a + E_L & J_{ab}^* & \mu_b^* \sqrt{n-1} \\ \mu_b \sqrt{n} & J_{ab} & E_b + E_L & \mu_a^* \sqrt{n-1} \\ 0 & \mu_b \sqrt{n-1} & \mu_a \sqrt{n-1} & E_a + E_b \end{pmatrix}, \quad (15)$$

$$\mathbf{B}_1^{(n)} = \begin{pmatrix} \mu^* \sqrt{n} & 0 \\ J^* & \mu^* \sqrt{n-1} \\ V^* & 0 \\ 0 & V^* \end{pmatrix}, \quad (16)$$

$$\mathbf{B}_2^{(n)} = \mathbf{B}_1^{(n)\dagger}, \quad (17)$$

$$\mathbf{K}^{(n)}(E_d) = \begin{pmatrix} E_d + E_L & \mu_a^* \sqrt{n-1} \\ \mu_a \sqrt{n-1} & E_a + E_d \end{pmatrix}. \quad (18)$$

We introduce the matrix

$$\mathbf{M}^{(n)} = \mathbf{A}^{(n)} - i\pi \mathbf{B}_1^{(n)} \mathbf{B}_2^{(n)}, \quad (19)$$

and let $\xi_1^{(n)}$ and $\xi_2^{(n)}$ denote the eigenvalues of the matrix $\mathbf{K}^{(n)}(0)$ and $\Lambda_{\mathbf{M}^{(n)j}}^{(n)}$, $j = 1, 2, 3, 4$, be the eigenvalues of the matrix $\mathbf{M}^{(n)}$. Let us recall the possibility of decompositions

$$\mathbf{K}^{(n)}(0) = \xi_1^{(n)} \mathbf{K}_1^{(n)} + \xi_2^{(n)} \mathbf{K}_2^{(n)}, \quad (20)$$

$$\mathbf{M}^{(n)} = \sum_{j=1}^4 \Lambda_{\mathbf{M}^{(n)j}}^{(n)} \mathbf{M}_j^{(n)}, \quad (21)$$

where $\mathbf{K}_1^{(n)}$, $\mathbf{K}_2^{(n)}$ are solutions of the equations

$$\begin{aligned}
\mathbf{K}_1^{(n)} + \mathbf{K}_2^{(n)} &= \mathbf{I}_2, \\
\xi_1^{(n)} \mathbf{K}_1^{(n)} + \xi_2^{(n)} \mathbf{K}_2^{(n)} &= \mathbf{K}^{(n)}(0). \quad (22)
\end{aligned}$$

Similarly, $\mathbf{M}_j^{(n)}$, $j = 1, 2, 3, 4$, are solutions of the equations

$$\sum_{j=1}^4 \Lambda_{\mathbf{M}^{(n)j}}^{(n)k} \mathbf{M}_j^{(n)} = \mathbf{M}^{(n)k}, \quad k = 0, 1, 2, 3. \quad (23)$$

In Eqs. (22) and (23), \mathbf{I}_2 and $\sum_{j=1}^4 \mathbf{M}_j^{(n)} = \mathbf{I}_4$ are 2×2 and 4×4 unit matrices, respectively.

The first vector of the components of the solution of Eqs. (13) has the very simple form

$$\mathbf{c}^{(n)}(t) = \exp\left(-\frac{i}{\hbar} \mathbf{M}^{(n)} t\right) \mathbf{c}^{(n)}(0). \quad (24)$$

We introduce a 2×4 matrix $\mathbf{T}^{(n)}(E_d)$ as the solution of the Sylvester equation

$$\mathbf{K}^{(n)}(E_d) \mathbf{T}^{(n)}(E_d) - \mathbf{T}^{(n)}(E_d) \mathbf{M}^{(n)} = \mathbf{B}_2^{(n)}. \quad (25)$$

The solution has the form

$$\mathbf{T}^{(n)}(E_d) = \sum_{k=1}^2 \sum_{j=1}^4 \frac{\mathbf{K}_k^{(n)} \mathbf{B}_2^{(n)} \mathbf{M}_j^{(n)}}{E_d + \xi_k^{(n)} - \Lambda_{\mathbf{M}^{(n)j}}^{(n)}}. \quad (26)$$

The dependence of the components of the amplitude spectrum on the initial state of the system with $\mathbf{d}^{(n)}(E_d, 0) = \mathbf{0}$ is

$$\begin{aligned}
\mathbf{d}^{(n)}(E_d, t) &= \left\{ \exp\left[-\frac{i}{\hbar} \mathbf{K}^{(n)}(E_d) t\right] \mathbf{T}^{(n)}(E_d) \right. \\
&\quad \left. - \mathbf{T}^{(n)}(E_d) \exp\left[-\frac{i}{\hbar} \mathbf{M}^{(n)} t\right] \right\} \mathbf{c}^{(n)}(0). \quad (27)
\end{aligned}$$

We observe that

$$\mathbf{d}^{(n)}(E_d, t) \simeq \mathbf{d}_{\text{out}}^{(n)}(E_d, t) \quad \text{for } t \rightarrow \infty, \quad (28)$$

where

$$\mathbf{d}_{\text{out}}^{(n)}(E_d, t) = \exp\left[-\frac{i}{\hbar} \mathbf{K}^{(n)}(E_d) t\right] \mathbf{T}^{(n)}(E_d) \mathbf{c}^{(n)}(0). \quad (29)$$

The increase of the diagonal terms by $2E_L$ means that also the eigenvalues $\xi_k^{(n)}$, $k = 1, 2$, $\Lambda_{Mj}^{(n)}$ are raised by the same amount. In the relations like (26), these increments mutually cancel and elsewhere they already correspond to the relation (11).

All the previous exposition beginning with (14) should be modified for $n < 2$. Let us note that the initial vacuum field and the ground states of the atoms a and b , $n = 0$, do not lead to any transitions to the continuum states. It holds that $\mathbf{c}^{(0)}(t) = (c_{00}^{(0)}(t))$ and the description reduces to the equation $\frac{d}{dt}c_{00}^{(0)}(t) = -\frac{i}{\hbar}2E_Lc_{00}^{(0)}(t)$. The reduction for $n = 1$ is a consequence of non-existence of $|n-2\rangle_L$ as in (11) and need not be made explicit. Let us note that transition to a continuum state can occur for $n = 1$, but not simultaneously with an excitation of the atom a .

III. NUMERICAL RESULTS

The long-time behavior is characterized by a complete ionization of the atom with an auto-ionizing level and by both the levels of the two-level atom a being occupied. The long-time behavior is periodical due to the dynamics of the two-level atom in the cw laser field. At all times the spectra can be determined as the probability distribution of the two-level atom at its levels and of the atom with the auto-ionizing level in the continuum of levels. By the normalization, conditional spectra are defined. The difference between the conditional spectra is an effect of the atomic quantum correlation. The difference between the conditional spectra can be seen even in the case where the dipole-dipole interaction of the atoms is missing.

An important case of the quantum correlation is the entanglement. We measure this entanglement using the negativity. The entanglement is conserved, even though we restrict the continuum of levels to two of them, in the most of the pairs of the selected frequencies. We calculate the negativity of the partially transposed statistical matrix for two levels of the two-level atom and selected continuum levels of the atom with an auto-ionizing level.

A. Appropriate parametrization

In the previous work, the functions

$$q_b = \frac{\mu_b}{\pi V^* \mu}, \quad \gamma_b = \pi |V|^2 \quad (30)$$

of the parameters of the atom b without a neighbor have been conveniently introduced. Also the functions

$$q_a = \frac{\mu_a}{\pi J^* \mu}, \quad \gamma_a = \pi |J|^2 \quad (31)$$

of the parameters of both the atoms have been defined. Here we conveniently introduce a one-photon version of the usual 'excitation' parameter Ω ,

$$\Omega = \sqrt{4\pi\Gamma(Q^2 + 1)}\mu, \quad (32)$$

where

$$\Gamma = \gamma_a + \gamma_b, \quad Q = \frac{\gamma_a q_a + \gamma_b q_b}{\Gamma}. \quad (33)$$

By the replacements $\mu_b \rightarrow J_{ab}$, $\mu \rightarrow J$ in the function q_b , the function

$$q_{\text{trans}} = \frac{J_{ab}}{\pi V^* J} \quad (34)$$

originates. For $V, J \geq 0$, the parameters of the model can be expressed in the forms

$$V = \sqrt{\frac{\gamma_b}{\pi}}, \quad J = \sqrt{\frac{\gamma_a}{\pi}}, \quad \mu = \frac{\Omega}{\sqrt{4\pi\Gamma(Q^2 + 1)}}, \\ \mu_a = \pi J^* \mu q_a, \quad \mu_b = \pi V^* \mu q_b, \quad J_{ab} = \pi V^* J q_{\text{trans}}. \quad (35)$$

From this, $q_a, \gamma_a, q_b, \gamma_b, \Omega, q_{\text{trans}}$ are new parameters.

In what follows, we will assume $E_a = E_b = E_L = 1$ and four different physically interesting cases that elucidate the behavior of the analyzed system:

- (a) $q_a = 0; \gamma_a = 0; q_b = \gamma_b = 1; \Omega = 0.1, 1; q_{\text{trans}} = 0$,
- (a') $q_a = 100; \gamma_a = 0; q_b = \gamma_b = 1; \Omega = 0.1, 1; q_{\text{trans}} = 0$,
- (b) $q_a = 100; \gamma_a = 10^{-4}; q_b = \gamma_b = 1; \Omega = 0.1; q_{\text{trans}} = 0$,
- (c) $q_a = 100; \gamma_a = 10^{-4}; q_b = \gamma_b = 1; \Omega = 0.1; q_{\text{trans}} = 1$.

Whereas atom b is alone in (a), it feels the presence of atom a due to the quantized optical field in (a'). In (b), both atoms interact by the dipole-dipole interaction that includes only the continuum of states at the atom b . Finally, also the dipole-dipole interaction between the discrete levels of both atoms is taken into play in (c). We note that detuning of energy levels of both atoms from the laser frequency does not qualitatively modify the behavior of the system (for more details, see [17] for semiclassical model). Also, we analyze the system at time $t = 2$ bellow. For the considered values of parameters, the behavior of the system at time $t = 2$ already corresponds to that appropriate to the long-time limit.

B. The role of atom a in forming the ionization spectra

In the model, atoms a and b are in fact mutually coupled by two types of interactions. Side by side with the discussed dipole-dipole interaction, the interaction mediated by photons in the quantized field also occurs. This interaction qualitatively distinguishes the presented fully quantum model from the common semiclassical models that assume a classical predefined optical pump field [11, 12].

The long-time limit of the two atomic systems is described by a statistical matrix $(\rho_{jk}^{\text{out}}(E_d, E'_d, t))$, with two discrete indices j, k and two continuous arguments E_d, E'_d . Here

$$\rho_{jk}^{\text{out}}(E_d, E'_d, t) \\ = \sum_{n=\max(1+j, 1+k)}^{\infty} d_{j_{\text{out}}}^{(n-1-j)}(E_d, t) d_{k_{\text{out}}}^{(n-1-k)*}(E'_d, t). \quad (36)$$

As usual, the photoelectron spectra are identified with the distributions

$$W_j^{\text{out}}(E_d, t) = \rho_{jj}^{\text{out}}(E_d, E_d, t), \quad j = 0, 1. \quad (37)$$

This joint description may be reduced to the marginal probability distribution of the levels of the atom a ,

$$p_j^{\text{out}}(t) = \int_{-\infty}^{\infty} W_j^{\text{out}}(E_d, t) dE_d. \quad (38)$$

We consider also the conditional distributions or spectra

$$W_{|j}^{\text{out}}(E_d, t) = \frac{W_j^{\text{out}}(E_d, t)}{p_j^{\text{out}}(t)}, \quad j = 0, 1. \quad (39)$$

The closed formula for $p_j^{\text{out}}(t)$ is rather complicated,

$$p_j^{\text{out}}(t) = \sum_{n=1+j}^{\infty} \int_{-\infty}^{\infty} \left| d_{j\text{out}}^{(n-1-j)}(E_d, t) \right|^2 dE_d, \quad (40)$$

where

$$\begin{aligned} & \int_{-\infty}^{\infty} \left| d_{j\text{out}}^{(n-1-j)}(E_d, t) \right|^2 dE_d \\ &= \left(\int_{-\infty}^{\infty} \mathbf{d}_{\text{out}}^{(n)}(E_d, t) \mathbf{d}_{\text{out}}^{(n)\dagger}(E_d, t) dE_d \right)_{jj}, \end{aligned} \quad (41)$$

with

$$\begin{aligned} & \int_{-\infty}^{\infty} \mathbf{d}_{\text{out}}^{(n)}(E_d, t) \mathbf{d}_{\text{out}}^{(n)\dagger}(E_d, t) dE_d = 2\pi \\ & \times \sum_{k=1}^2 \sum_{j=1}^4 \sum_{k'=1}^2 \sum_{j'=1}^4 \frac{\exp \left[\frac{i}{\hbar} (\xi_{k'}^{(n)} - \xi_k^{(n)}) t \right]}{i \left(\xi_{k'}^{(n)} - \xi_k^{(n)} - \Lambda_{\mathbf{M}^{(n)}j'}^* + \Lambda_{\mathbf{M}^{(n)}j} \right)} \\ & \times \mathbf{K}_k^{(n)} \mathbf{B}_2^{(n)} \mathbf{M}_j^{(n)} \mathbf{c}^{(n)}(0) \mathbf{c}^{(n)\dagger}(0) \mathbf{M}_{j'}^{(n)\dagger} \mathbf{B}_1^{(n)} \mathbf{K}_{k'}^{(n)}. \end{aligned} \quad (42)$$

The long-time total photoelectron spectrum is time-independent,

$$W^{\text{out}}(E_d) = W_0^{\text{out}}(E_d, t) + W_1^{\text{out}}(E_d, t). \quad (43)$$

In Figs. 2 and 3 the case (a') of data with $\Omega = 0.1$ and for the initial coherent state $|1\rangle_L$ is illustrated. The unconditioned and conditional photoelectron spectra have a multi-peak structure and the peak positions are about the same for both the values of the subscript j . Therefore the plot is restricted to an interval which includes a single peak of a spectrum. In Fig. 2, it is seen that the unconditioned photoelectron spectra coincide and cannot be discerned in the chosen interval. In contrast, in Fig. 3 it is obvious that the conditional spectra differ significantly in the selected interval. It proves the dependence of the occupation of the atom b 's level on the atom a 's level.

To reveal the role of atom a in ionization of atom b , we compare the long-time ionization spectra of atom b for

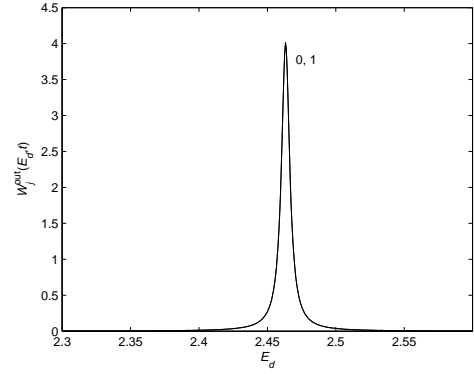


FIG. 2: Unconditioned photoelectron spectra $W_j^{\text{out}}(E_d, t)$, $t = 2$, $j = 0, 1$. Initially the laser mode is in a coherent state with the mean photon number equal to 1. The photon energy is $E_L = 1$. The energy differences $E_b = E_a = 1$. The parameters $q_a = 100$, $\gamma_a = 0$, $q_b = \gamma_b = 1$, $\Omega = 0.1$, $q_{\text{trans}} = 0$.

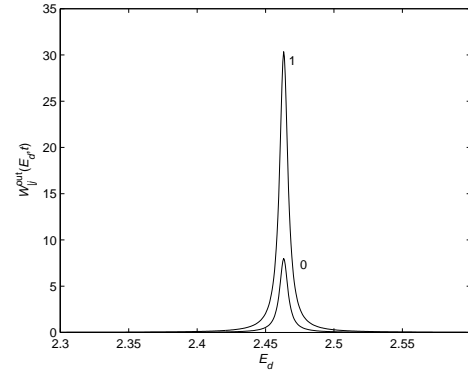


FIG. 3: Same as in Fig. 2, but the conditional spectra $W_{|j}^{\text{out}}(E_d, t)$, $j = 0, 1$, are plotted.

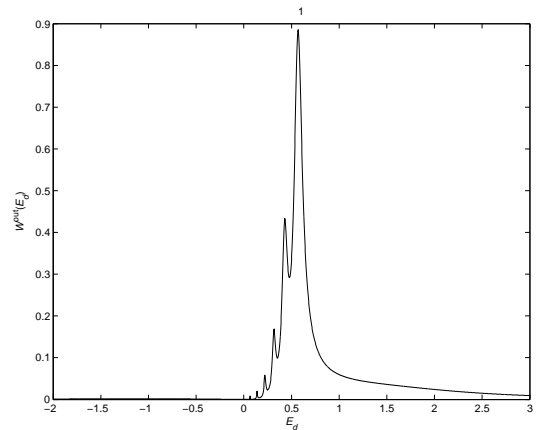


FIG. 4: Photoelectron spectrum $W^{\text{out}}(E_d)$. Initially the laser mode is in a coherent state with the mean photon number equal to 1. The parameters $E_a = E_b = E_L = 1$, $q_a = 0$, $\gamma_a = 0$, $q_b = \gamma_b = 1$, $\Omega = 1$, $q_{\text{trans}} = 0$.

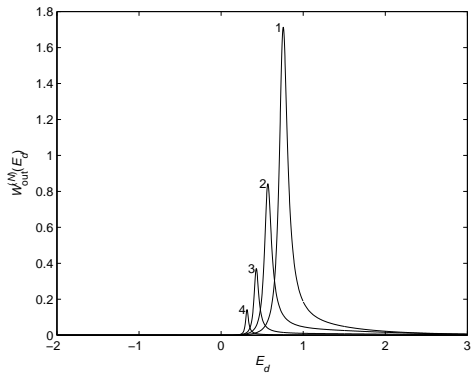


FIG. 5: Fock components $W_{\text{out}}^{(N)}(E_d)$, $N = 1, \dots, 4$, of the spectrum $W^{\text{out}}(E_d)$. The parameters are the same as in Fig. 4.

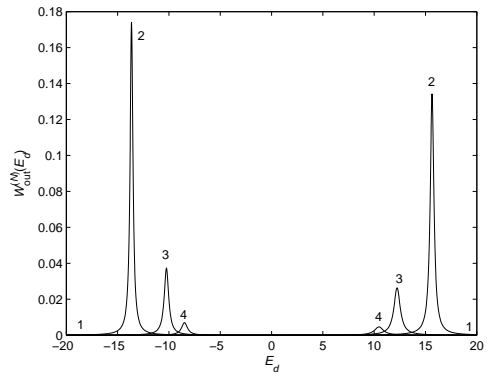


FIG. 7: Fock components $W_{\text{out}}^{(N)}(E_d)$, $N = 1, \dots, 4$, of the spectrum $W^{\text{out}}(E_d)$. The parameters are the same as in Fig. 4, but the parameter $q_a = 100$.

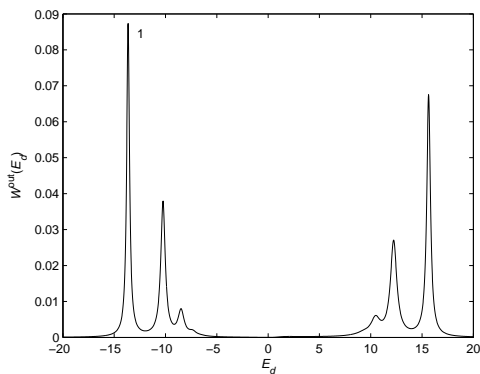


FIG. 6: Photoelectron spectrum $W^{\text{out}}(E_d)$. The parameters are the same as in Fig. 4, but the parameter $q_a = 100$.

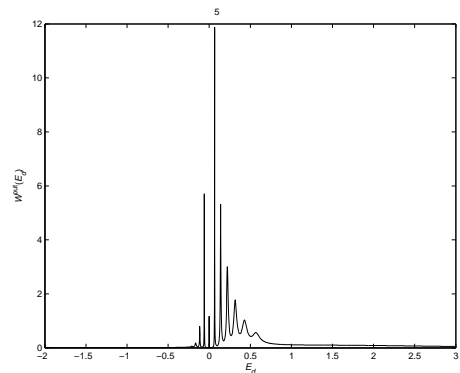


FIG. 8: Photoelectron spectra $W^{\text{out}}(E_d)$. The parameters $E_a = E_b = E_L = 1$, $\gamma_a = 0$, $q_b = \gamma_b = 1$, $\Omega = 1$, $q_{\text{trans}} = 0$. Here the initial mean photon number is equal to 5, $q_a = 0$.

atom a present and absent. We consider a greater value of single-photon Rabi frequency Ω to emphasize quantum features of the model ($\Omega = 1$).

Ionization of isolated atom b in a quantized field leads, in general, to the occurrence of sharp peaks in the ionization spectra (see Fig. 4). These peaks arise from the ionization caused by individual Fock states of the optical field. This is documented in Figs. 4, 5, in which the ionization spectra corresponding to the coherent and Fock states are shown. It holds that the greater the Fock number n is, the narrower is the corresponding spectral peak and also the closer is the peak to the position of energy of the Fano zero (see Fig. 4). Such behavior qualitatively resembles that of an ionization spectrum caused by a classical strong pump field [5].

The presence of atom a in the quantized pump field considerably modifies the ionization spectra of atom b due to the mutual indirect interaction of both atoms through the quantized pump field. Contrary to the spectra of isolated atom b , the ionization spectra have contributions both below and above the pump-field frequency. Moreover, the spectral peaks above and below the pump-field frequency occur in pairs which results in nearly sym-

metric ionization spectra (see Figs. 6, 7). This symmetry is inherent to the Fock states from which it transfers into the coherent states, as documented in Figs. 6, 7. It holds that the greater the Fock number n , the closer the two peaks to the pump-field frequency.

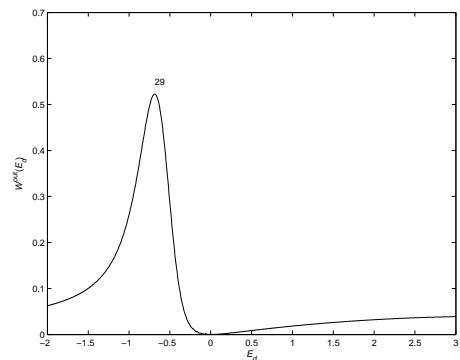


FIG. 9: Same as in Fig. 8, but the initial mean photon number is equal to 29, $q_a = 0$.

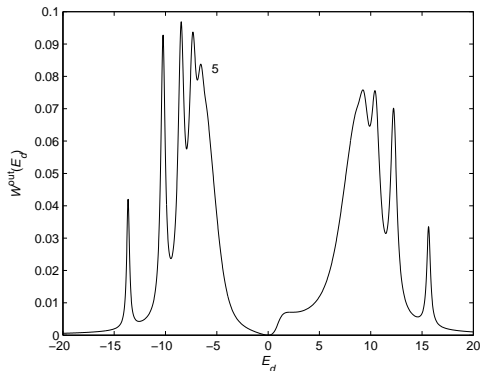


FIG. 10: Same as in Fig. 8, but the initial mean photon number is equal to 5, $q_a = 100$.

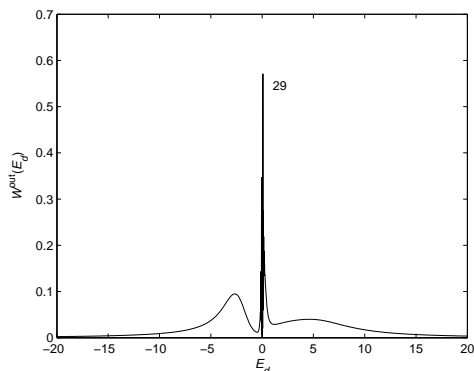


FIG. 11: Same as in Fig. 8, but the initial mean photon number is equal to 29, $q_a = 100$.

If the pump-field intensity increases, the spectrum of isolated atom b is built more and more from contributions of higher-number Fock states and it moves to lower energies crossing the energy of Fano zero. The more intense the pump field, the more suppressed (smoothed) the spectral structure of individual Fock states (see Figs. 8, 9). Also the narrowing of the overall ionization spectrum in the vicinity of the energy of Fano zero is observed. When atom a is present, the ionization spectra also gradually lose their peaked structure with the increasing pump-field intensities (see Figs. 10, 11). For sufficiently high pump-field intensities, the spectrum approaches that of the isolated atom a .

When the interaction mediated by the quantized field is weaker, the behavior of ionization spectra with the increasing pump-field intensities is qualitatively similar to the usual one discussed in the Fano model. The spectra move towards lower energies with the increasing pump-field intensities and cross at certain intensity the energy of Fano zero, as documented in Figs. 12, 13. Whereas the isolated atom b has a one-peak spectrum, the spectrum of atom b influenced by atom a consists of two peaks that form a spectral doublet at greater pump-field intensities

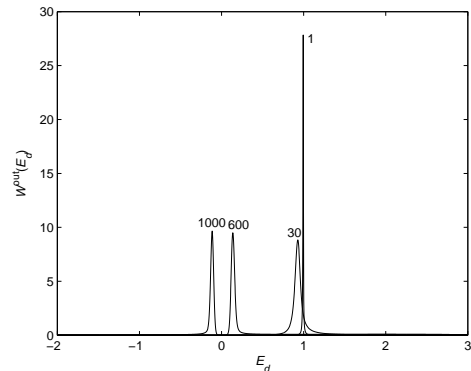


FIG. 12: Photoelectron spectra $W^{\text{out}}(E_d)$. Initially the laser mode is in coherent states with the mean photon numbers equal to 1, 30, 600, 1000. The parameters $E_a = E_b = E_L = 1$, $\gamma_a = 0$, $q_b = \gamma_b = 1$, $\Omega = 0.1$, $q_{\text{trans}} = 0$. Here $q_a = 0$.

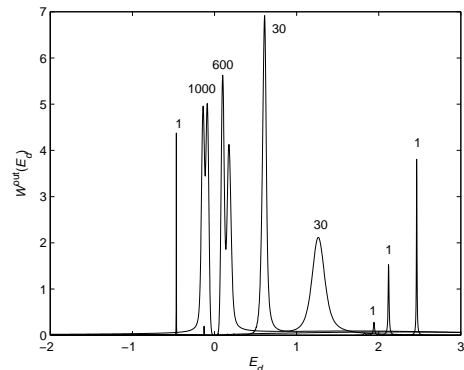


FIG. 13: Same as in Fig. 12, but $q_a = 100$.

clearly visible in Fig. 13.

C. Ionization spectra formed by the dipole-dipole interaction

The dipole-dipole interaction between atoms a and b , in general, splits the peaks in the ionization spectra of isolated atom b into two parts (see Figs. 14, 15, 16). As a consequence, there occur two major peaks in the ionization spectra for greater pump-field intensities. These spectral peaks are broken into many sub-peaks for low pump-field intensities as a consequence of quantum character of the pump field (see Fig. 14). Individual sub-peaks can be connected with the appropriate Fock states, similarly as in the previous section. Two major peaks approach each other with the increasing pump-field intensity and form a spectral doublet at certain moment (see Fig. 15).

If only the dipole-dipole interaction between the discrete level of atom a and the continuum of states of atom b ($J \neq 0$) is considered, the Fano zero of isolated atom b

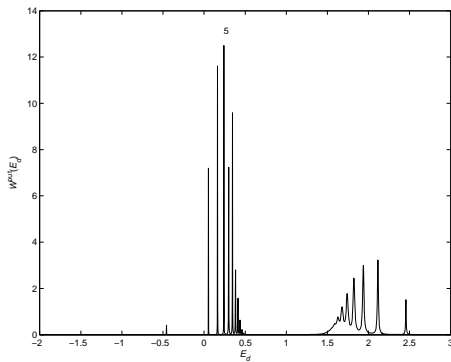


FIG. 14: Photoelectron spectra $W^{\text{out}}(E_d)$. The parameters $E_a = E_b = E_L = 1$, $q_a = 100$, $\gamma_a = 10^{-4}$, $q_b = \gamma_b = 1$, $\Omega = 0.1$, $q_{\text{trans}} = 0$. Initially the laser mode is in a coherent state with the mean photon number equal to 5.

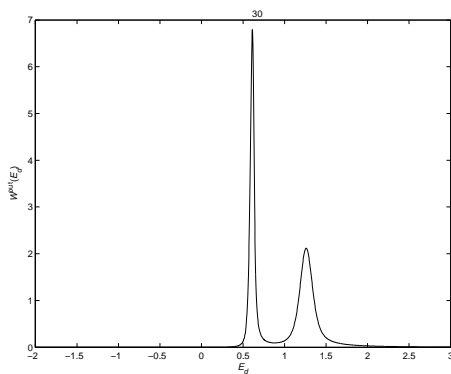


FIG. 15: Same as in Fig. 14, but with the mean photon number equal to 30.

is inevitably lost. However, when also the dipole-dipole interaction between the discrete levels of atoms a and b occurs ($J_{ab} \neq 0$), the Fano zero can be preserved under certain conditions found in [13]. The two mentioned dipole-dipole interactions compete in ionizing atom b in certain sense. If the strengths of two interactions equal

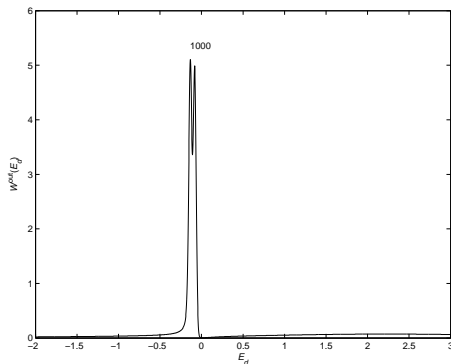


FIG. 16: Same as in Fig. 14, but with the mean photon number equal to 1000.

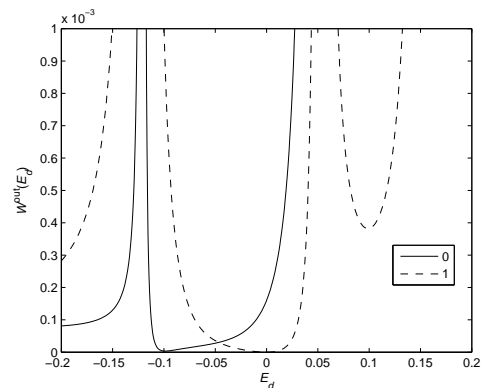


FIG. 17: Photoelectron spectra $W^{\text{out}}(E_d)$. Initially the laser mode is in a coherent state with the mean photon number equal to 3. The parameters $E_a = E_b = E_L = 1$, $q_a = 100$, $\gamma_a = 10^{-4}$, $q_b = \gamma_b = 1$, $\Omega = 0.1$, $q_{\text{trans}} = 0$ (solid curve), 1 (dashed curve).

for the energy of Fano zero formed at atom b , the Fano zero is preserved. The appropriate condition was derived in [13] for the semi-classical model in the form

$$\frac{J_{ab}}{J} = \frac{\mu_b}{\mu}. \quad (44)$$

Numerical computations have revealed that the condition in Eq. (44) is valid also in the analyzed quantum model (see Fig. 17). Here, we would like to note that the original Fano zero of isolated atom b is usually replaced by a broad deep minimum in the ionization spectra provided that the condition in Eq. (44) is not fulfilled (see Fig. 17). Such behavior originates in the weakness of dipole-dipole interactions compared to the Coulomb and optical dipole interactions that form the Fano zero of isolated atom b .

D. Entanglement of atoms a and b

We have assessed the entanglement by the 'computable measure of entanglement', i. e., the negativity [18]. It is recommended as such in the case of two parties (components) each possessing a finite number of levels. We mark a difference, because in our analysis one of the two parties has an infinite number of levels. The straightforward approach was successful on the assumption of a classical light field [17], because the two components are in a joint pure quantum state. To our knowledge, such an approach cannot be based on simple formulas on inclusion of the quantum nature of the field which leads to a mixed quantum state describing the involved parties. Numerical calculation would be a challenging task.

Recently, a selection of the frequencies has been realized in a somewhat arbitrary, but systematic, way [17]. Two states with these frequencies are just the levels needed for producing a qubit. In such a way, we return to the well-known two-qubit problem. For $E_d, E'_d \in [-2, 3]$,

$[-20, 20], [-5, 10], [-1.5, 1.5]$, we generate a 'density' plot of the negativity at $t = 2$ that is

$$\mathcal{N}(t) = \sum_{l=1}^4 \frac{|\bar{\lambda}_l(t)| - \bar{\lambda}_l(t)}{2}, \quad (45)$$

where $\bar{\lambda}_l(t)$ are eigenvalues of the partially transposed statistical matrix

$$\begin{pmatrix} \rho_{00}^{\text{out}}(E_d, E_d, t) & \rho_{00}^{\text{out}}(E_d, E'_d, t) & \rho_{10}^{\text{out}}(E_d, E_d, t) & \rho_{10}^{\text{out}}(E_d, E'_d, t) \\ \rho_{00}^{\text{out}}(E'_d, E_d, t) & \rho_{00}^{\text{out}}(E'_d, E'_d, t) & \rho_{10}^{\text{out}}(E'_d, E_d, t) & \rho_{10}^{\text{out}}(E'_d, E'_d, t) \\ \rho_{01}^{\text{out}}(E_d, E_d, t) & \rho_{01}^{\text{out}}(E_d, E'_d, t) & \rho_{11}^{\text{out}}(E_d, E_d, t) & \rho_{11}^{\text{out}}(E_d, E'_d, t) \\ \rho_{01}^{\text{out}}(E'_d, E_d, t) & \rho_{01}^{\text{out}}(E'_d, E'_d, t) & \rho_{11}^{\text{out}}(E'_d, E_d, t) & \rho_{11}^{\text{out}}(E'_d, E'_d, t) \end{pmatrix}. \quad (46)$$

Here

$$\begin{aligned} & \begin{pmatrix} \rho_{jk}^{\text{out}}(E_d, E_d, t) & \rho_{jk}^{\text{out}}(E_d, E'_d, t) \\ \rho_{jk}^{\text{out}}(E'_d, E_d, t) & \rho_{jk}^{\text{out}}(E'_d, E'_d, t) \end{pmatrix} \\ &= \frac{1}{\sum_{j=0}^1 [\rho_{jj}^{\text{out}}(E_d, E_d, t) + \rho_{jj}^{\text{out}}(E'_d, E'_d, t)]} \\ & \times \begin{pmatrix} \rho_{jk}^{\text{out}}(E_d, E_d, t) & \rho_{jk}^{\text{out}}(E_d, E'_d, t) \\ \rho_{jk}^{\text{out}}(E'_d, E_d, t) & \rho_{jk}^{\text{out}}(E'_d, E'_d, t) \end{pmatrix}, \end{aligned} \quad (47)$$

with

$$\begin{aligned} \rho_{jk}^{\text{out}}(E_d, E_d, t) &= \rho_{jk}^{\text{out}}(E_d, E'_d, t)(E'_d \rightarrow E_d), \\ \rho_{jk}^{\text{out}}(E'_d, E_d, t) &= \rho_{jk}^{\text{out}}(E_d, E'_d, t)(E_d \leftrightarrow E'_d), \\ \rho_{jk}^{\text{out}}(E'_d, E'_d, t) &= \rho_{jk}^{\text{out}}(E_d, E'_d, t)(E_d \rightarrow E'_d), \\ j, k &= 0, 1. \end{aligned} \quad (48)$$

Both the dipole-dipole interaction and the interaction mediated by the quantized pump field create the entanglement between the bound electron at atom a and the ionized electron at atom b . Suitable conditions for creating highly entangled states have been revealed in [17] concerning a classical pump field. It holds that the stronger the dipole-dipole interaction, the more entangled state is reached. However, also a weaker dipole-dipole interaction can provide highly entangled states provided that the ionization process is sufficiently slow. This can be reached when the strengths of the direct ionization path (connecting the ground state of atom b with the continuum) and the indirect ionization path (that ionizes an electron from the ground state of atom b through the auto-ionizing discrete state of atom b) are balanced.

Similarly as in the semiclassical model analyzed in [17], the overall negativity can roughly be composed of negativities of qubit-qubit systems obtained from the qubit of atom a and all possible qubits found in the continuum of atom b . Such densities of negativity give us information about the spectral distribution of entanglement. The density of negativity for the ionization spectrum shown in Fig. 6 and appropriate for the interaction mediated by the quantized field is plotted in Fig. 18. We can see in Fig. 18 that the negativity is distributed in the whole area of energies present in the ionization spectrum. It is remarkable that the values of density of negativity are very low for the degenerate energies of qubits inside the

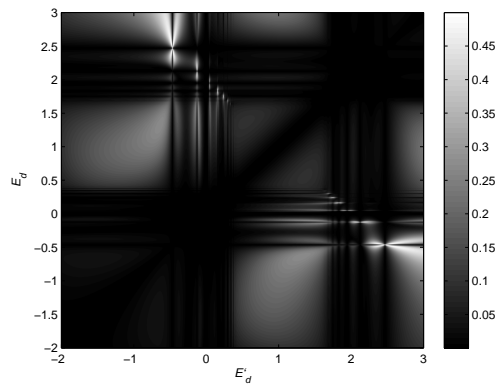


FIG. 18: Density plot of the negativity \mathcal{N} ($t = 2$) that measures the entanglement between the neighbor atom a and the atom b with a continuum. The parameters $E_a = E_b = E_L = 1$, $q_a = 100$, $q_b = \gamma_b = 1$, $\Omega = 0.1$, $q_{\text{trans}} = 0$. Initially, the laser mode is in a coherent state with the mean photon number equal to 1, $\gamma_a = 0$.

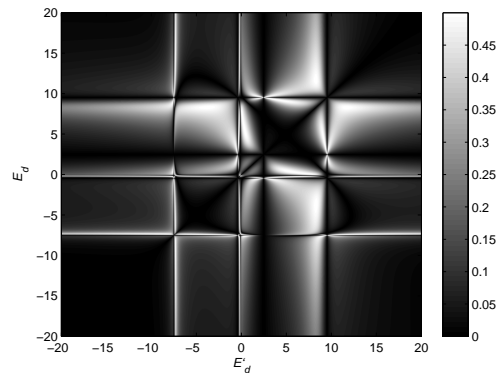


FIG. 19: Same as in Fig. 18, but initially, the laser mode is in the Fock state $|2\rangle_L$, $\gamma_a = 10^{-4}$.

continuum of atom b ($E_d \approx E'_d$). This behavior can be explained by the long-time energy conservation that does not allow to entangle such qubits in the continuum with the qubit of atom a . The densities of negativity appropriate to the coherent and Fock states completely differ, as demonstrated in Figs. 18, 19. We note that a pump field in the Fock state with one photon cannot create entanglement due to the energy conservation. However, higher-number Fock states are already suitable for the entanglement creation.

The densities of negativities formed by the dipole-dipole interaction behave similarly as those created by the interaction mediated by the quantized field. It holds also here that appreciable values of the density of negativity are found for energies appreciably present in the ionization spectra. Also very low values of the density of negativity occur around the degenerate energies $E_d \approx E'_d$ (see Figs. 20, 21). Thus, the spectral concentration of negativity is observed as the pump-field intensity

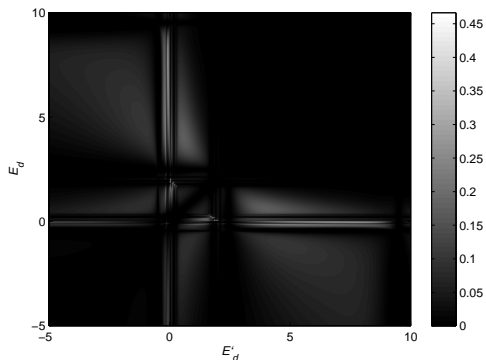


FIG. 20: Same as Fig. 18, but $\gamma_a = 10^{-4}$.

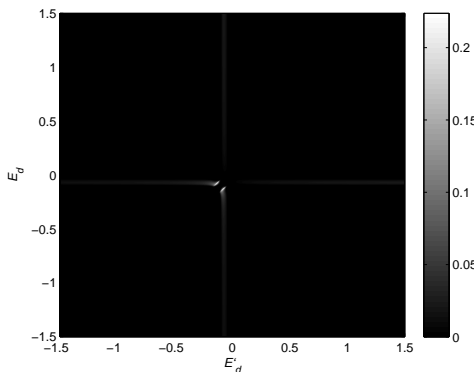


FIG. 21: Same as Fig. 18, but the initial mean photon number is equal to 1000, $\gamma_a = 10^{-4}$.

increases (compare Figs. 20, 21). When the spectrum forms a spectral doublet, the entanglement is encoded between the two peaks of the doublet.

As follows from the above results, effects stemming from quantum features of the pump optical field are clearly visible both in ionization spectra and entanglement provided that the one-photon 'excitation' parameter Ω is greater or comparable to 0.1 and the mean number of photons is smaller or comparable to 10. Both coherent laser fields and highly-nonclassical Fock-state fields are suitable for the observation of quantum signa-

tures of auto-ionization process. As for the Fock-state fields, they can be generated, e.g., in heralded single-photon sources [19] or their generalizations [20] and in QED cavities [21]. Greater values of the one-photon 'excitation' parameter Ω represent experimental challenge as the values reached in current ionization experiments are much smaller. However, modern photonic band-gap structures [22, 23] give a hope here. They allow to dramatically increase electric-field amplitudes inside due to constructive interference on one side. On the other side, they form photonic bands with continuum of states which are similar to those participating in ionization.

IV. CONCLUSIONS

We have studied quantum correlations of two atoms. We have assumed that one atomic system contains an auto-ionizing level whereas the other atom does not comprise any auto-ionizing level. Both the atoms interact with the same mode of the quantized field. We have concentrated ourselves to the long-time behavior of the atomic systems. The long-time behavior exhibits quantum correlations of the two atoms even in the case where the atoms do not interact directly. We have illustrated quantum correlations comparing the one-peak spectrum appropriate for the neighbor atom without optical excitation with the two-peak spectrum occurring for the optically-excited neighbor atom. In the classical limit of strong field the differences vanish. **We have identified conditions for the observation of quantum features in long-time electron ionization spectra.** Also the Fano zero has been found in these spectra for the quantized optical field considering the same conditions as for the classical optical field.

Acknowledgments

The authors acknowledge the financial support by the project Operational Program Research and Development for Innovations - European Social Fund (project CZ.1.05/2.1.00/03.0058) of the Ministry of Education, Youth and Sports of the Czech Republic and the project IGA No. PrF-014-05.

[1] U. Fano, Phys. Rev. **124**, 1866 (1961).
 [2] U. Fano and J. W. Cooper, Phys. Rev. **137**, A1364 (1965).
 [3] P. Rehmus and R. S. Berry, Phys. Rev. A **23**, 416 (1981).
 [4] P. Lambropoulos and P. Zoller, Phys. Rev. A **24**, 379 (1981).
 [5] K. Rzażewski and J. H. Eberly, Phys. Rev. Lett. **47**, 408 (1981).
 [6] W. Leoński, R. Tanaś, and S. Kielich, J. Opt. Soc. Am. B **4**, 72 (1987).
 [7] W. Leoński and V. Bužek, J. Mod. Opt. **37**, 1923 (1990).

[8] W. Leoński, J. Opt. Soc. Am. B **10**, 244 (1993).
 [9] A. E. Miroshnichenko, S. Flach, and Y. S. Kivshar, Rev. Mod. Phys. **82**, 2257 (2010).
 [10] A. Lukš, V. Peřinová, J. Peřina, Jr., J. Křepelka, and W. Leoński, in *Wave and Quantum Aspects of Contemporary Optics*, edited by J. Müllerová, D. Senderáková, and S. Jurečka, Proceedings of SPIE Vol. 7746 (Bellingham: SPIE) p 77460W (2010).
 [11] J. Peřina, Jr., A. Lukš, W. Leoński, and V. Peřinová, Phys. Rev. A **83**, 053416 (2011).
 [12] J. Peřina, Jr., A. Lukš, W. Leoński, and V. Peřinová,

- Phys. Rev. A **83**, 053430 (2011).
- [13] J. Peřina, Jr., A. Lukš, V. Peřinová, and W. Leoński, *Opt. Express* **19**, 17133–17142 (2011).
- [14] J. Peřina, Jr., A. Lukš, V. Peřinová, and W. Leoński, *J. Russian Laser Res.* **32**, 212 (2011).
- [15] B. Najjari, A. B. Voitkiv, and C. Müller, *Phys. Rev. Lett.* **105**, 153002 (2010).
- [16] A. B. Voitkiv and B. Najjari, *Phys. Rev. A* **82**, 052708 (2010).
- [17] A. Lukš, J. Peřina, Jr., W. Leoński, and V. Peřinová, *Phys. Rev. A* **85**, 012321 (2012).
- [18] G. Vidal, R. F. Werner, *Phys. Rev. A* **65**, 032314 (2002).
- [19] G. Brida, I. P. Degiovanni, M. Genovese, F. Piacentini, P. Traina, A. Della Frera, A. Tosi, A. Bahgat Shehata, C. Scarcella, A. Gulinatti, M. Ghioni, S. V. Polyakov, A. Migdall, and A. Giudice, *Appl. Phys. Lett.* **101**, 221112 (2012).
- [20] J. Peřina Jr., O. Haderka and V. Michálek, *Opt. Express* **21**, 19387 (2013).
- [21] B. T. H. Varcoe, S. Brattke and H. Walther, *New J. Phys.* **6**, 97 (2004).
- [22] J. D. Joannopoulos, S. G. Johnson, J. N. Winn, and R. D. Meade, *Photonic Crystals: Molding the Flow of Light* (Princeton University Press, Princeton, 2011), 2nd ed.
- [23] K. Sakoda, *Optical Properties of Photonic Crystals*, (Springer, New York, 2005).